TKK Dissertations 213
Espoo 2010

DYNAMICS OF SHIP COLLISIONS

Doctoral Dissertation

Kristjan Tabri

Aalto University
School of Science and Technology
Faculty of Engineering and Architecture
Department of Applied Mechanics

TKK Dissertations 213
Espoo 2010

DYNAMICS OF SHIP COLLISIONS

Doctoral Dissertation

Kristjan Tabri

Dissertation for the degree of Doctor of Science in Technology to be presented with due permission of the Faculty of Engineering and Architecture for public examination and debate in Auditorium K216 at the Aalto University School of Science and Technology (Espoo, Finland) on the 9th of February, 2010, at 12 noon.

Aalto University
School of Science and Technology
Faculty of Engineering and Architecture
Department of Applied Mechanics

Aalto-yliopisto
Teknillinen korkeakoulu
Insinööritieteiden ja arkkitehtuurin tiedekunta
Sovelletun mekaniikan laitos

Distribution:
Aalto University
School of Science and Technology
Faculty of Engineering and Architecture
Department of Applied Mechanics
P.O. Box 15300
FI - 00076 Aalto
FINLAND
URL: http://appmech.tkk.fi
Tel. +358-9-470 23501
Fax +358-9-470 24173
E-mail: leila.silonsaari@aalto.fi

ISBN 978-952-248-272-3
ISBN 978-952-248-273-0 (PDF)
ISSN 1795-2239
ISSN 1795-4584 (PDF)
URL: http://lib.tkk.fi/Diss/2010/isbn9789522482730/

TKK-DISS-2723

Multiprint Oy
Espoo 2010

ABSTRACT OF DOCTORAL DISSERTATION	HELSINKI UNIVERSITY OF TECHNOLOGY P.O. BOX 1000, FI-02015 TKK http://www.tkk.fi

Author Kristjan Tabri

Name of the dissertation
Dynamics of Ship Collisions

Manuscript submitted 30.09.2009	Manuscript revised 10.12.2009

Date of the defence 09.02.2010

☐ Monograph ☒ Article dissertation (summary + original articles)

Faculty Faculty of Engineering and Architecture
Department Department of Applied Mechanics
Field of research Naval Architecture
Opponent(s) Professor Preben Terndrup Pedersen
Supervisor Professor Petri Varsta
Instructor Professor Jerzy Matusiak

The thesis studies ship collisions computationally and experimentally on large and model scales. On the basis of the experimental observations a 3D simulation model is proposed that couples the motions of the ships to the contact force, and considers all the major hydromechanical forces that act on colliding ships. Additionally, the effects of sloshing and the dynamic bending of the hull girder are investigated and implemented into the simulation model.

Large-scale experiments were analysed in order to get a deeper insight into the collision dynamics. On the basis of the large-scale experiments a model-scale test setup is designed using the Froude's scaling law. There, the emphasis was laid on the external dynamics and the structural response, properly scaled from the large-scale test, was modelled using homogeneous foam in the side structure of the struck ship model. It is shown that the model-scale experiments illustrated the large-scale tests both qualitatively and quantitatively. A wide range of symmetric, both with and without sloshing, and non-symmetric collision scenarios are studied on a model scale.

The experimental findings are exploited in the development of a coupled collision simulation model. The model is formulated in three-dimensional space, and the contact force between the colliding ships considers both the normal and frictional components. A discrete mechanical model for sloshing is implemented into this time-domain model. This linear sloshing model describes the fluid in partially filled tanks with a single rigid mass and with a number of oscillating mass elements that interact with the ship structure through springs and dampers. The dynamic bending of the ship hull girder is included by modelling it as an Euler-Bernoulli beam.

Both the experiments and the simulations emphasised the importance of the coupling between the motions and the contact force. It was especially obvious in the case of non-symmetric collisions and in the experiments with sloshing. The penetration paths calculated with the developed time-domain simulation model agreed well with those from the experiments. The total deformation energy was predicted with a deviation of about 10%. The hydrodynamic radiation forces acting on colliding ships proved to have a strong influence on the energy distribution as at the end of the contact they accounted for up to 25% of the total available energy. However, if the interest is in the maximum deformation, the approach with the hydrodynamic damping ignored yields an error of about 5% in the deformation energy. The results of the large- and model-scale experiments with partially filled liquid tanks emphasised the importance of sloshing for collision dynamics. The structural deformation energy in the tests with sloshing was only about 70%-80% of that in similar collision tests without sloshing. The simulation method with the linear sloshing model overestimated the deformation energy by up to 10% for low filling levels of water, but in the case of medium filling levels the predictions agreed amazingly well.

Keywords ship collisions, model-scale experiments, large-scale experiments, water sloshing

ISBN (printed) 978-952-248-272-3	ISSN (printed) 1795-2239
ISBN (pdf) 978-952-248-273-0	ISSN (pdf) 1795-4584
Language English	Number of pages 51+60

Publisher Helsinki University of Technology, Department of Applied Mechanics

Print distribution Helsinki University of Technology, Department of Applied Mechanics

☒ The dissertation can be read at http://lib.tkk.fi/Diss/ 2010/isbn9789522482730/

Preface

This thesis is based on work done at the Schelde Naval Shipyard during 2003-2004 and at the Department of Applied Mechanics, Helsinki University of Technology during 2004-2009. During the thesis process I was financed within the framework of the Marie Curie Intra-European Fellowship programme, by the Finnish National Graduate School of Engineering Mechanics, the Finnish National project TÖRMÄKE, and the EU-funded research project MARSTRUCT, and by the Finnish Maritime Foundation. This financial support is greatly acknowledged.

I wish to express my sincere gratitude to my supervisor, Professor Petri Varsta, for his continuous support and encouragement during the course of this work. His guidance was crucial and helped me overcome many obstacles I encountered in my research work. I would also like to thank my instructor, Professor Jerzy Matusiak, whose knowledge and sense of exactness contributed significantly to the scientific quality of the thesis. I am very grateful to Professor Jaan Metsaveer from Tallinn University of Technology for his long support and for introducing me to Naval Architecture. Special thanks are due to Leila Silonsaari, whose support and help with daily matters is highly appreciated.

I would like to take this opportunity to honour Mr. J.W.L. Ludolphy, who was the initiator of the cooperation between the Schelde Naval Shipyard and Helsinki University of Technology in the framework of the Marie Curie Intra-European Fellowship programme. His involvement made it possible to obtain valuable experimental data and to gain an insight into a more practical approach to ship collision problems. He passed away unexpectedly on 22 September 2002. The guidance and long discussions with my co-workers, Joep Broekhuijsen, Jan Jaap Nieuwenhuis, Marcel Elenbaas, Rob de Gaaij, and Bob van de Graaf at the Schelde Naval Shipyard were valuable and inspiring, especially during the earlier stages of the research work.

I would also like to thank my colleagues in the Ship Laboratory, Heikki Remes, Jani Romanoff, Sören Ehlers, Alan Klanac, Jasmin Jelovica, Pentti Kujala and Pentti Tukia, for their support and helpfulness, and for creating a pleasant working atmosphere. I greatly appreciate the support and friendship of my Estonian colleagues D.Sc. Hendrik

Naar and Meelis Mäesalu. Special thanks go to my dear friends from Otaniemi for the fantastic and unforgettable times we spent together.

Finally, I am deeply grateful to my parents for their irreplaceable support and devotion. Last but not least, I thank my dear Kaia-Liisa for bringing immeasurable happiness into my life and for being supportive throughout the whole thesis process.

Helsinki, January 2010 Kristjan Tabri

Contents

Appendix

[P1] Tabri K., Broekhuijsen J., Matusiak J., Varsta P. (2009) Analytical modelling of ship collision based on full-scale experiments. Journal of Marine Structures, 22(1), pp. 42-61.

[P2] Tabri K., Määttänen J., Ranta J. (2008) Model-scale experiments of symmetric ship collisions, Journal of Marine Science and Technology, 13, pp. 71-84.

[P3] Tabri K., Varsta P., Matusiak J. (2009) Numerical and experimental motion simulations of non-symmetric ship collisions, Journal of Marine Science and Technology, doi: 10.1007/s00773-009-0073-2.

[P4] Tabri K., Matusiak J., Varsta P. (2009) Sloshing interaction in ship collisions – An experimental and numerical study, Journal of Ocean Engineering, 36, pp. 1366-1376.

List of Symbols

$a(\omega)$	frequency-dependent added mass
a, b, c	parameters defining the elliptical paraboloid
A_L	lateral area
A, B, C	parameters defining the plane
$\mathcal{A}$	area
$b(\omega)$	frequency-dependent added damping
B	ship's breadth
c_n	damping coefficient of the nth damped mass-spring element
C_y	drag coefficient
[C]	damping matrix
D	depth
E	energy
E_B	bending energy
E_C, E_D	deformation energy
E_F	work against the friction force
E_K, E_{KIN}	kinetic energy
E_{SL}	sloshing energy
EI	flexural stiffness
F	force and moment vector
F_C	contact force
F_E	external excitation force in the sloshing model
F_F	fluid force in sloshing model
F_H	hydrodynamic radiation force
F_I	inertial force
F_K	velocity-dependent component of the radiation force
F_M	total force resulting from sloshing
F_n	Froude number
F_p	compressive force in the contact model
F_q	frictional force in the contact model

F_R	restoring force
F_μ	inertial component of the radiation force; viscous shear force
g	gravity
h	height; vertical distance; water depth;
h_W	water height
I	number of partially filled tanks; moment of inertia
J	total number of degrees of freedom associated with oscillating masses
k_n	stiffness of the nth mass-spring element
k	stiffness; radii of inertia
K	sum of roll moments acting on the ship; retardation function,
[K], [**K**]	stiffness matrix
[$\mathbf{K}_\mathrm{b}$]	matrix of retardation functions
l_T	dimension of the tank in the sloshing direction
L	length
m_i^*	generalised mass of ith mode
$m_{x,}\, m_{y,}\, m_z$	sum of ship's and its added mass in the x-, y-, and z- directions
m_n	nth oscillating mass-spring element in sloshing model
m_R	a single rigid sloshing mass in a tank
$\hat{m}_R$	sum of rigid sloshing masses
m_T	total fluid mass in a tank
m_{ST}	structural mass
M	sum of pitch moments; ship mass including added mass
[M] or [**M**]	mass matrix
$\left[\mathbf{M}_\mu^\Omega\right]$	matrix of non-linear acceleration and added mass, structural mass and inertia terms
n	normal
N	number of oscillating masses per tank
N_R	number of rigid degrees of freedom
p,q,r	angular velocities
p	pressure; normal coordinate (in vibrations); normal traction

$\mathcal{P}$	plane
Q	total number of degrees of freedom
q	distributed loading; tangential traction
q_i^*	generalised loading associated with *i*th mode shape
r	position vector
R	position vector
R_N	Reynolds number
$\mathcal{S}$	surface
t	time
T	ship's draught
[**T**]	matrix of transformation
$\mathcal{T}$	tangent plane
u	surge velocity at ship's centre
u	vector of translational velocity
v	sway velocity at ship's centre, velocity in general
V_0	initial velocity of a sloshing tank
V_F	final velocity of a sloshing tank
w	heave velocity at ship's centre
W	work
x_n	displacement of the *n*th oscillating mass-spring element in the sloshing model
x_R	displacement of the rigid mass in the sloshing model
$x^i y^i z^i$	local coordinate systems (i=*A, B*)
$x^0 y^0 z^0$	inertial coordinates
X, Y, Z	sum of forces acting on the ship in the longitudinal, transverse, and vertical directions
β	collision angle
γ	pitch angle
δ	penetration; logarithmic decrement of damping

ε	restoring coefficient
η	horizontal vibration response of the hull girder
λ	scaling factor
$\boldsymbol{\lambda}_Q^A$	direction vector in the contact model
μ	non-dimensional added mass; viscosity
μ_d	coefficient of friction
ξ	damping ratio; internal damping of hull girder
ρ	density
σ	stress
τ	time parameter in retardation function, duration
φ	roll angle
$[\boldsymbol{\varphi}]$	column matrix of Euler's angles
ψ, θ, ϕ	Euler's angles
ϕ	natural mode
ω	frequency
$\boldsymbol{\Omega}$	vector of rotational velocity
∇	volumetric displacement of the ship

Superscripts

0	inertial coordinate system
A	striking ship
B	struck ship
M	model-scale
S	ship-scale

Subrscripts

0	initial
E	elastic
F	fluid (force)
G	gravitational (force)

H	radiation (force)
i	ith vibratory mode; index
K	retardation (force or energy)
n	nth sloshing mass; denotes sloshing matrices
P	plastic
SL	sloshing
μ	added mass

Abbreviations

dof	degree of freedom
VOF	volume of fluid
CFD	computational fluid dynamics
LED	light-emitting diode
KG	vertical height of the centre of gravity
COG	centre of gravity

List of publications and Author's Contribution

This thesis consists of an introductory report and the following four papers:

[P1] Tabri K., Broekhuijsen J., Matusiak J., Varsta P. (2009) Analytical modelling of ship collision based on full-scale experiments. Journal of Marine Structures, 22(1), pp. 42-61.

The author gave a quantitative description of large-scale collision experiments in which sloshing interaction on ships was included. The manuscript was prepared by the author. Broekhuijsen provided large-scale experimental data. Matusiak and Varsta made valuable recommendations concerning the development of the theory and contributed to the manuscript.

[P2] Tabri K., Määttänen J., Ranta J. (2008) Model-scale experiments of symmetric ship collisions, Journal of Marine Science and Technology, 13, pp. 71-84.

The author designed the test setup, validated its physical similarity to the large-scale collision experiments, conducted the final analysis, and prepared the manuscript. Määttänen took part in designing the test setup, conducted the experiments, and provided the initial analysis of the results. Ranta studied the modelling of structural resistance and provided the geometry of the impact bulb to ensure dynamic similarity to the large-scale tests.

[P3] Tabri K., Varsta P., Matusiak J. (2009) Numerical and experimental motion simulations of non-symmetric ship collisions, Journal of Marine Science and Technology, doi: 10.1007/s00773-009-0073-2.

The author developed the theory and carried out the calculations and the validation. The manuscript was prepared by the author. Varsta made recommendations on the development of the contact model and contributed to the manuscript. Matusiak contributed to the external dynamics model and to the manuscript.

[P4] Tabri K., Matusiak J., Varsta P. (2009) Sloshing interaction in ship collisions – An experimental and numerical study, Journal of Ocean Engineering, 36, pp. 1366-1376.

The author designed the test setup and conducted the experiments and the development and validation of the simulation model. The manuscript was prepared by the author. Matusiak and Varsta provided valuable comments and contributed to the manuscript.

Original Features

Ship collisions are a complex phenomenon as they consist of transient ship motions and structural deformations, commonly referred to as external dynamics and internal mechanics. The majority of collision simulation models decouple the external dynamics from the inner mechanics for the sake of simplicity. This thesis proposes a coupled simulation model considering all six degrees of freedom for both colliding ships. The ships are regarded as being rigid when their global motions are being considered. An allowance for major local structural deformations is made when dealing with the contact between the ships. The following features of this thesis are believed to be original.

1. The distribution of energy components during large-scale collision experiments was calculated and presented in [P1]. These distributions present the quantitative significance of different energy-absorbing mechanisms in ship collisions and reveal the important phenomenon of sloshing.
2. A model-scale test setup for ship collisions was designed and scaled according to the large-scale tests in [P2]. It was shown in [P2] that the model-scale tests were physically similar to the large-scale ones. The test setup was exploited to investigate collision dynamics in symmetric [P2] and non-symmetric collisions [P3].
3. An experimental study on sloshing interaction in collision dynamics was performed. The interaction was studied on a large scale in [P1] and on a model scale for a wide range of collision scenarios in [P4].
4. A three-dimensional ship collision model, including the coupling between external dynamics and inner mechanics, was developed with the help of the kinematic condition [P3]. This condition is based on the mutual ship motions and on the geometry of the colliding ships, giving the penetration and, thus, the contact force. The elastic springback of structures deformed in a collision was considered during the separation of the ships. The simulation model was validated with the help of the experimental results of the symmetric collision tests in [P1] and those of the non-symmetric collision test in [P3].

5. The effects of fluid sloshing in partially filled tanks are included in the simulation model, using a discrete mechanical model for sloshing [P1 & P4]. The vibratory response of the hull girder of the struck ship is included for the sway motion of the struck ship [P1].

1. Introduction

1.1. Background

Waterborne vehicles have been subject to a variety of accidents since their early dawn. With the increasingly higher speeds and displacements of ships, the consequences of accidents could be disastrous. Today's society is more reluctant to accept environmental damage and casualties. Therefore, significant marine accidents, for example the collision of the Stockholm and Andrea Doria in 1956 or the grounding of the Exxon Valdez in 1989, have often formed a basis for the development of measures to increase the safety of shipping. Operational safety measures aim to reduce the probability of accidents occurring, while structural safety measures in ships concentrate on the reduction of the consequences. Regardless of the measures developed, accidents involving ships can never be completely avoided – human errors, technical malfunctions, or other unpredictable events continue to occur. Eliopoulou and Papanikolaou (2007) studied the statistics of tanker accidents and showed that the total number of accidents and the number of accidents causing pollution has decreased significantly in recent decades. However, the accidents causing pollution have not decreased to the same extent as the overall number of accidents. It has become obvious that the safety measures to reduce the consequences in accidents, such as ship collisions or groundings, should still be improved.

A reduction of the consequences of ship collisions implies the ability of colliding structures to absorb energy without a rupture causing flooding or oil spillage. The structure's ability to withstand collisions is collectively called crashworthiness. A crashworthiness analysis of ship structures combines two separate fields, external dynamics and inner mechanics (Minorsky, 1959). The external dynamics evaluates the ship motions, giving as a result the energy to be absorbed by structural deformations, while the inner mechanics evaluates the deformations the structures undergo while absorbing that energy. The first studies on the crashworthiness of ship structures date back to the 1950s and deal with the collision safety of nuclear-powered ships. The understanding of the physics involved was based on facts learned from actual collision accidents (Minorsky, 1959) or on simplified experiments on the inner mechanics

(Woisin 1979). Mainly because of the seriousness of the possible consequences, early crashworthy structures implemented in nuclear-powered ships such as the NS Savannah or NS Otto Hahn (see Soininen (1983) for the structural principles) were, however, far too impractical to be implemented in typical commercial ships. A significant improvement in crashworthiness came with the introduction of double-bottomed and, later, double-hulled tankers. Spacious double walls provide an additional buffer zone between the intruding object and the inner compartments of the ship. Knowledge about the performance of these structures was based on large-scale structural tests in the laboratory (Woisin, 1979; Amdahl and Kavlie, 1992). In recent decades many research studies have been devoted to developing even more efficient and compact crashworthy structures, for example a Y-core side structure (Ludolphy and Boon, 2000) or a buffer bow (Kitamura, 2000).

Figure 1. Large-scale collision experiment in the Netherlands (photo taken by the author).

The performance of the novel Y-core structure was studied, together with other concepts, in a series of large-scale experiments (Carlebur, 1995; Wevers & Vredeveldt, 1999); see Figure 1. There, collisions between two river tankers with displacements of an order of magnitude of 1000 tons were studied. These were the first collision experiments that also included the external dynamics and its coupling to the inner mechanics. The analysis of the experiment with the Y-core side structure revealed

shortcomings in the understanding of collision phenomena. Contrary to the predictions made beforehand, the structure that was tested did not tear and was only slightly damaged (Broekhuijsen, 2003). Not only the way in which the structure deformed, but also the amount of energy to be absorbed was significantly lower compared to the predictions. In addition to the contact and the hydromechanical forces, there were other mechanisms absorbing a significant part of the available energy. Possible interactions arising from partially filled cargo tanks and from the dynamic bending of the hull had been excluded from the analysis. For the sake of brevity, we refer to these very relevant phenomena as complementary effects. These depend on the time histories of the ships' motions and on the contact force. The motions should be calculated in parallel to the structural deformations to account for possible mutual interaction, i.e. the coupling between the inner mechanics and the external dynamics has to be considered on a reasonable level.

The decoupling is possible in symmetric ship collisions, where the striking ship collides at a right angle with the amidships of the struck ship and where the complementary effects are negligible. In such a collision the ship motions are limited to a few components and the contact force as a function of the penetration can be predefined. The actual extent of the penetration is obtained by comparing the area under the force-penetration curve to the deformation energy from the external dynamics. Statistical studies (Lützen, 2001; Tuovinen, 2005) have, however, indicated that the majority of collisions are non-symmetric in one way or another. Often the collision angle deviates from 90 deg or the contact point is not at the amidships. In non-symmetric ship collisions the penetration path cannot be predefined with reasonable precision, but it should be evaluated in parallel with the ship motions, implying once again the need for a coupled approach. Model-scale experiments (Määttänen, 2005) provide a first insight into the dynamics of non-symmetric collisions. These tests, together with the large-scale experiments, make it possible to develop and validate a coupled approach to ship collision simulations, including all the relevant energy-absorbing mechanisms.

1.2. State of The Art

One of the first calculation models to describe the external dynamics of ship collisions was proposed by Minorsky (1959). This single-degree-of-freedom (dof) model was based on the conservation of linear momentum and there was no coupling with the inner mechanics. The interaction between the ship and the surrounding water was through a constant added mass. The model allowed fast estimation of the energy available for structural deformations without providing exact ship motions. Woisin (1988) extended the collision model to consider three dof – surge, sway and yaw. Later, in 1998, Pedersen and Zhang included the effects of sliding and elastic rebounding. These two-dimensional (2D) models in the plane of the water surface are capable of analysing non-symmetric collisions and evaluating the loss of kinetic energy in a collision absorbed by structural deformations. However, there only the inertial forces are taken into account and thus, the effects of several hydromechanical force components and the contact force are neglected.

Minorsky's assumption of the constant added mass was investigated experimentally by Motora et al. (1971). In their experiments a ship model was pulled sideways with a constant force. They concluded that the constant value of the added mass is a reasonable approximation only when the duration of the contact and the transient motion is very short. A more precise method of presenting this so-called hydrodynamic radiation force was proposed by Cummins (1962) and Ogilvie (1964). Their method draws a clear distinction between two components of the force; one component is proportional to the ship's acceleration and the other is a function of her velocity. The first of these components is what is described with the constant added mass term. The velocity-dependent component, commonly referred to as the hydrodynamic damping force, accounts for the memory effects of water. This approach requires the evaluation of frequency-dependent added mass and damping coefficients, which can be obtained by experiments (Vugts, 1968), by numerical methods (Journee, 1992), or by algebraic expressions based on a conformal mapping solution (Tasai, 1961). In 1982, Petersen suggested a procedure for the time-domain simulations of ship collisions in which the hydrodynamic forces were included, as suggested by Cummins (1962) and Ogilvie (1964). Ship motions were again limited to the horizontal plane of

the water. This approach was validated with the model tests of Motora et al. (1971) and good agreement was found.

As far as the author knows, the model of Petersen (1982) was the first time-domain simulation model capable of treating non-symmetric collisions in 2D. Earlier time-domain simulation models by Drittler (1966) and Smiechen (1974) required either preliminary knowledge of the ship motions or were limited to symmetric collision scenarios. In Petersen's model the coupling between the motions and the structural deformations was included quasi-statically using non-linear springs. Therefore, the component of the contact force arising as a result of the relative velocity between the ships, i.e. the frictional force, was disregarded. Brown (2002) described a similar coupled approach and also included the frictional force between the ships. Still, the hydrodynamic forces were considered only through the constant added mass. He compared the calculated deformation energy to that evaluated with the decoupled approach of Pedersen and Zhang (1998). It was concluded that, while the total deformation energy was predicted well, the decoupled method results in a different decomposition of the total deformation energy in the transverse and longitudinal directions, compared to that given by the coupled method.

Le Sourne at al. (2001) formulated the external dynamics of collisions in a three-dimensional (3D) space considering six dof for global ship motions and, similarly to Petersen (1982), included the hydrodynamic forces on the basis of Cummins (1962) and Ogilvie (1964). The coupling between the ship motions and the structural deformations was carried out simultaneously with the help of structural analysis with the finite element method. The method was used to simulate an eccentric ship-submarine collision, where only small angular motions are excited during the contact. The analysis concentrated mainly on the motions after the contact and revealed the importance of the hydrodynamic damping force on the roll and yaw motion of the submarine.

As already discussed, the large-scale collision experiments (Carlebur, 1995; Wevers & Vredeveldt, 1999) revealed that the existing collision models did not explain all the possible energy-absorbing mechanisms. Tabri et al. (2004) included the sloshing model of Graham and Rodriguez (1952), and were the first to present the importance of sloshing interaction in collision dynamics. This sloshing model was also solved by

Konter et al. (2004), applying the finite element method. Sloshing in collisions was also studied by Zhang and Suzuki (2007), applying the arbitrary Lagrangian-Eulerian method. They concluded that for deep filling levels of water a simple mechanical model, similar to that of Graham and Rodriguez (1952), tends to overestimate the energy involved in sloshing motion.

The energy consumption resulting from the vibratory bending of the hull girder in collisions has been studied by Tabri et al. (2004) and Pedersen and Li (2004). Both studies revealed that the energy consumption in relation to the other absorbing mechanisms was small.

1.3. Scope of work

The present investigation comprises both an experimental and theoretical study; see Figure 2. Ship collisions are studied experimentally on a large and on a model scales. On the basis of the experimental observations, a 3D simulation model is proposed that couples the motions to the contact force, and considers all the major hydromechanical forces that act on the colliding ships. This makes it possible to carry out the simulations needed for the case of non-symmetric collisions. Additionally, the effects of sloshing and the dynamic bending of the hull girder are investigated and implemented into the simulation model.

Large-scale experiments were analysed in order to get a deeper insight into the collision dynamics [P1]. This study was published in the year 2004 in the form of an un-reviewed conference paper by Tabri et al. (2004). However, the data from the large-scale experiments covered a limited range of symmetric collision scenarios and, in particular, no information was obtained about non-symmetric collisions. Therefore, a model-scale test setup was designed on the basis of these large-scale experiments, using the Froude's scaling law to preserve geometric, dynamic, and kinematic similarity as far as possible. There, the emphasis is laid on the external dynamics. The structural response, properly scaled from the large-scale experiments, is modelled using homogeneous foam in the side structure of the struck ship model. This technique was adapted from model-scale ship grounding experiments (Lax, 2001). The crushing

resistance of the foam, together with a geometrically properly dimensioned impact bulb, gives a force-penetration curve similar to that in the large-scale tests. A wide range of symmetric and non-symmetric collision scenarios are studied on a model scale, allowing the influence of several parameters, such as the ships' masses, the collision velocity, the location of the contact point, the collision angle, and structural resistance to be investigated [P3 & P4]. Moreover, the sloshing effects are studied by filling the tanks on board the striking ship to different water levels [P4]. To improve the understanding of the sloshing interaction, these tests are repeated with equivalent fixed masses in tanks.

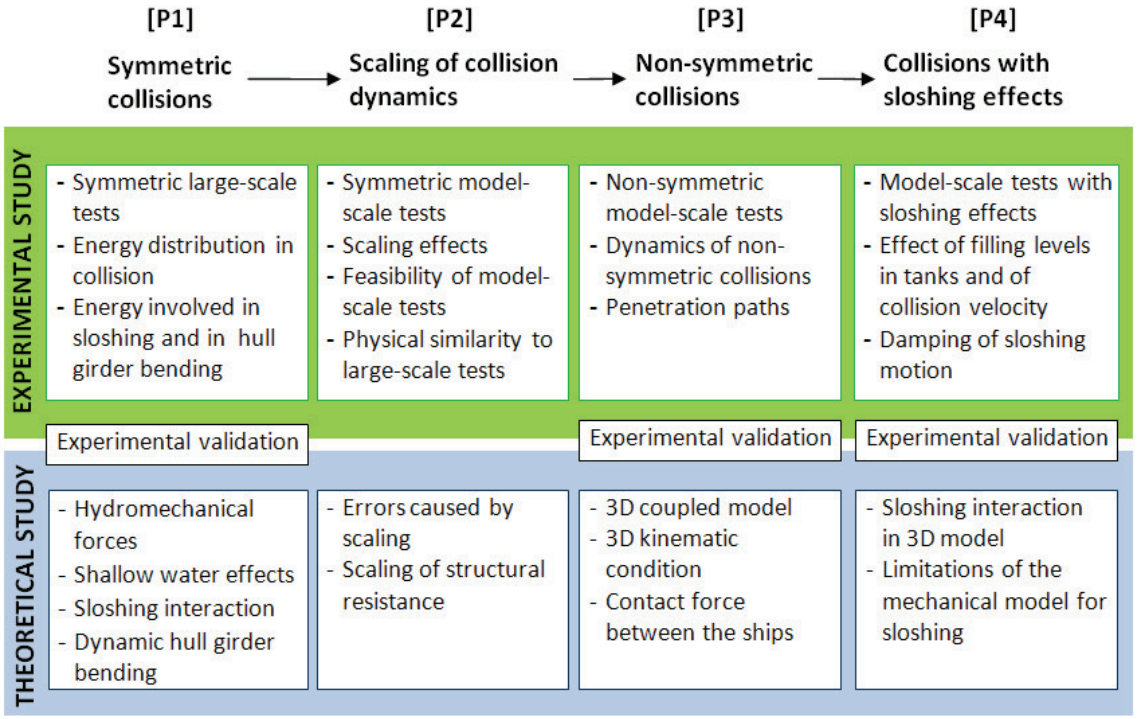

Figure 2. Outline of the investigation.

The experimental findings are exploited in the development of the coupled collision simulation model. The model is formulated in 3D, and the contact force between the colliding ships considers both the normal and frictional components [P3]. The formulation of the equations of motion follows the derivations by Clayton and Bishop (1982) and, in addition to this, the hydrodynamic radiation forces are evaluated using the theories of Cummins (1962) and Ogilvie (1964), together with the strip theory

(Journée, 1992). The kinematic condition between the colliding ships is served through a common contact force. The contact force is evaluated as an integral over normal and tangential tractions at the contact surface. The contact process is divided into three phases according to whether the penetration increases, remains constant, or decreases. During decreasing penetration the elastic springback of the deformed structures is considered.

The complementary effects, including the sloshing forces and the dynamic bending of the hull girder, are investigated both experimentally and computationally [P1 & P4]. Several symmetric collision scenarios are experimentally studied on a model scale to reveal the dynamics of sloshing. A discrete mechanical model for sloshing (Graham and Rodriguez, 1952) is implemented into the time-domain simulation model [P4]. This sloshing model provides a simple means to include the sloshing forces in a collision in the motion equations. It should be noticed that this model does not require precise and time-consuming numerical calculations. The sloshing model describes the fluid in partially filled tanks with a single rigid mass and with a number of oscillating mass elements that interact with the ship structure through springs and dampers. The dynamic bending of the ship hull girder is included by modelling it as an Euler-Bernoulli beam with a certain set of physical properties such as mass, flexural stiffness, and internal damping [P1].

1.4. Limitations

This thesis proposes a simulation model of ship collisions in which the approach to consider different phenomena involved, is kept simple for the sake of time efficiency. This sets certain limitations on the applicability of the model. These limitations are discussed below.

All the experiments and calculations are limited to collision scenarios where the struck ship is initially motionless. This is mainly due to the test setup of the model tests, where the focus was on the physical phenomena. The dynamics and kinematics involved with the forward speed of the striking ship are investigated. However, the physical principles remain the same for the struck ship in spite of possible interaction

resulting from the wave pattern arising from the surge of the struck ship also inducing a contact force component in that direction. The simulation model will not have this limitation, even though it lacks proper experimental validation. A calm sea is assumed throughout the experimental programme and the development of the simulation model.

The simulation model has both non-linear and linear features. Non-linearity arises from the contact force and linearity is related to hydromechanical forces such as the hydrostatic restoring force and the hydrodynamic radiation forces. Because of this, the roll angle of the ships is limited to angles of approximately 10°. Moreover, the hydrodynamic added mass and damping coefficients are calculated at the initial equilibrium position of the ships and the effect of the change in actual position and orientation is disregarded. These limitations are supported by the observations from the large- and model-scale experiments. Effects arising from wave patterns around the colliding ships and the hydrodynamic coupling between them are considered as being secondary and thus they are disregarded. Flooding and the ensuing loss of stability are not investigated as the time scale of a collision is small compared to these.

A study of the inner mechanics of ship side structures lies beyond the scope of the thesis as the focus is on collision dynamics. Therefore, in the study the side structure of the struck ship is replaced by homogeneous foam, with, however, the dynamic similarity being maintained. The calculation model for the contact force covers the kinematics between the ships and is based on the tractions at the contact surface described by the normal and tangential components, which are easily obtained for homogeneous material compared to that of real ship structures. The model is quasi-static, but includes friction forces based on the relative velocity between the ships.

The sloshing interaction is due to sway and surge, and angular motions play a minor role. The sloshing model applied in the simulations is based on linear flow theory and the effect of possible roof impacts is ignored. However, the damping effect is included with a simple viscous damping model.

The vibratory response of the hull girder is studied on a large scale, as in the model-scale experiments rigid ship models were used. In the simulation model the bending is considered as a vibratory response of the lowest eigenmode of an Euler-Bernoulli beam. This response is included only for the sway motion of the struck ship.

2. Experimental study

The collision dynamics were investigated through large- and model-scale experiments. The large-scale collision experiments (Wevers & Vredeveldt, 1999) provided an insight into symmetric collisions with sloshing interaction. The knowledge from the large-scale experiments is favourable as it is free of scaling effects, but on the other hand the tests are costly and thus a wide range of collision parameters cannot be studied. Model-scale experiments offer an alternative as a wider parametric range can be covered, but special attention has to be paid to scaling. A model-scale test setup was designed and validated with the help of the results of the large-scale experiments. In the model-scale tests a total of 46 collision experiments, including symmetric and non-symmetric collisions, were carried out. Further, the collision experiments with water sloshing were studied. For the sake of brevity, the experiments with water sloshing are henceforth referred to as "wet" tests, while the other experiments without sloshing phenomena are simply "dry" tests.

2.1. Large-scale experiments

Several full-scale collision experiments using two inland tankers were conducted in the Netherlands by TNO in the framework of a Japanese, German, and Dutch consortium (Wevers & Vredeveldt, 1999). These experiments had different purposes, such as to validate numerical analysis tools, to investigate collision physics, and to test new structural concepts. In this study the experiments with Y-core (Wevers & Vredeveldt, 1999) and X-core (Wolf, 2003) side structures are of interest.

In the Y-core experiment both the striking and the struck ships had large amounts of ballast water in partially filled tanks, providing the possibility of sloshing occurring during the collision. On the other hand, in the X-core experiment the possible sloshing effects were practically removed, as there was only a small amount of ballast water. On the basis of these experiments, the time histories of different energy components throughout the collision were evaluated in [P1] and the importance of sloshing phenomena was revealed on the basis of energy balance analysis. The observations and

measured results of the large-scale experiments provided basic knowledge for the design of the model-scale experiments and for the development of the simulation model.

2.2. Model-scale collision experiments

The model-scale experiments were performed to extend the physical understanding of ship collisions. The large-scale experiments were scaled to model scale using a scaling factor of 35 [P2]. The Froude scaling law was obeyed considering the practicalities of the experiments, such as reasonable magnitudes of velocities and forces involved in ship collision. This led to proper relation between inertia and gravity forces, while viscous forces were overestimated as a result of a too small Reynolds number. However, viscous forces have only a minor role in such a transient event as ship collision. As shown later in this chapter, the prevailing forces in ship collision are inertia forces together with the contact force.

The scaling resulted in ship models with the following main dimensions: length $L^A = L^B = 2.29$ m, depth $D^A = D^B = 0.12$ m, and breadth $B^A = 0.234$ m for the striking ship and $B^B = 0.271$ m for the struck ship. When compared on the same scale, the flexural rigidity of the ship models was significantly higher than that of the large-scale ships and thus, the hull girder bending was not studied on the model scale.

The striking ship model was equipped with a rigid bulb in the bow and it collided with the side structure of the struck ship model; see Figure 3. At the contact location a block of homogeneous polyurethane foam was installed. The force-penetration curve from the large-scale experiment was used to scale down the structural response of the struck ship and, thus, maintain dynamic similarity. The scaling was based on the crushing strength of the foam and on the geometry of the bulb [P2]. The selected foam had a crushing strength of 0.121 MPa (Ranta and Tabri, 2007).

The dry model-scale experiments were divided into three different sets on the basis of the collision scenario. The first set concentrated on symmetric collisions [P2], while the second and the third sets contained non-symmetric collision experiments [P3]. In the second set, the eccentricity L_C of the contact point was varied between $0.13L^B$ to $0.36L^B$ from the amidships towards the bow, but the collision angle β had the same value, 90°.

In the third set, the collision angles varied from 30° to 120°, but now the eccentricity was kept constant at around $\sim 0.18L^B$.

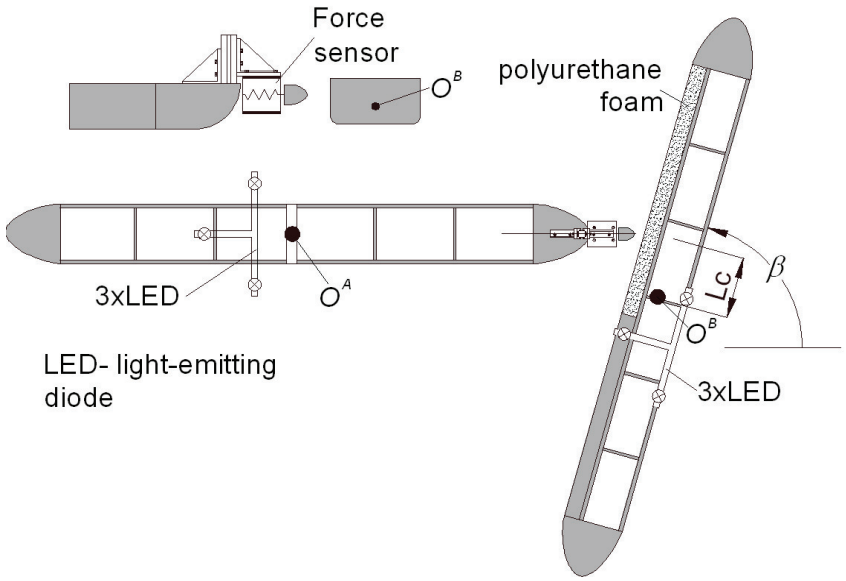

Figure 3. Model-scale test setup.

During the collision all six motion components of both ships were recorded with respect to an inertial coordinate system using a Rodym DMM non-contact measuring system. Depending on the collision scenario, the contact force was recorded either in a longitudinal or in the longitudinal and transverse directions with respect to the striking ship model. These two separate measuring systems were not synchronised because of a non-constant time lag resulting from the post-processing of data in the Rodym system. Thus, an automatic correction of the time lag was not possible and the synchronisation had to be carried out manually [P2].

The model-scale results of symmetric collisions, covering the motions, forces, and energy distributions, proved that the test setup provided results qualitatively and quantitatively similar to the large-scale tests [P2]. This fact made it possible also to exploit the results of the non-symmetric model-scale tests for the validation of the simulation model.

2.3. Model-scale collision experiments with sloshing effects

The sloshing phenomenon was experimentally studied on a model scale, with several water filling levels in two onboard tanks being considered [P4]. On the basis of the experience from the dry tests, the measuring systems were developed further to improve the synchronisation. In addition, two water tanks were installed on board the striking ship model; see Figure 4. The free surface elevation in the tanks was measured with four resistive wave probes made of steel wire. Three probes were installed in the fore tank and one in the aft tank.

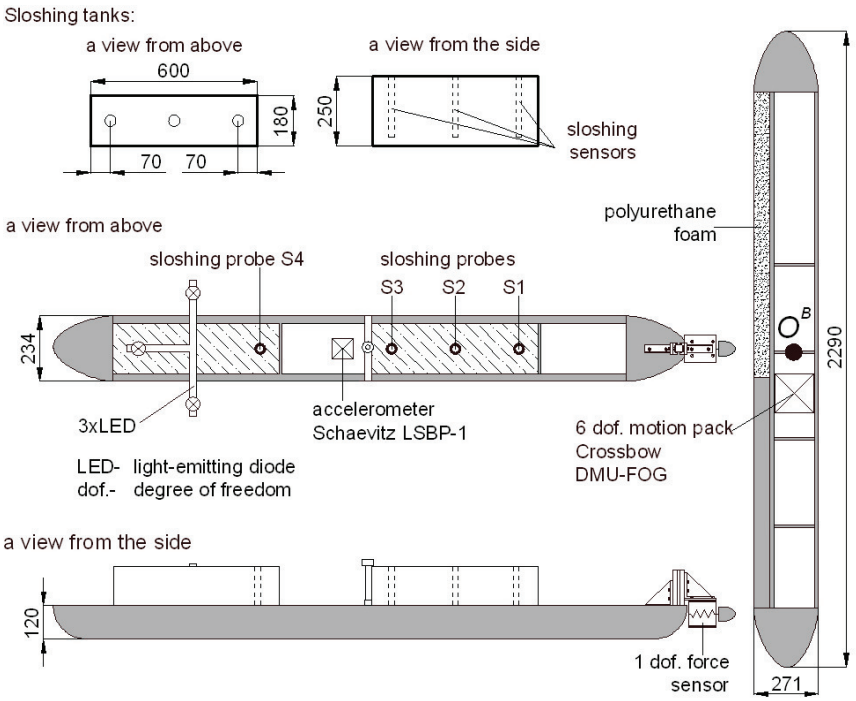

Figure 4. Model-scale test setup for wet tests.

Four different even-keel loading conditions of the striking ship model were tested under three velocities. The amount of water in the water tanks varied from 21% to 47% of the total displacement of the model. To deepen the understanding of the effect of the sloshing phenomena on collision dynamics, most of these wet tests were repeated with a loading condition in which the water in the tanks was replaced with rigid masses of the same weight.

The setup for the wet tests gave reliable and repeatable results [P4]. The results of the model-scale experiments clearly emphasised the importance of sloshing in connection with the collision dynamics. According to the results of the model experiments, it can be stated that the sloshing made the striking ship behave like a lighter ship, causing a reduction in the collision damage to the struck ship. This could be seen from the deformation energy, which in the wet tests was only about 80% of that in the dry tests with equivalent collision scenarios. This energy reduction value was clearly influenced by the filling level, but not that strongly by the initial collision velocity of the striking ship.

3. Collision dynamics

3.1. Physical phenomena of ship collisions

When two ships collide, the contact force arises as a result of the penetration of structures, defined as a relative position between the striking and the struck ship. The contact force causes the ships to become displaced from their current position. At any time instant the force has to be in balance with the inertial and hydromechanical forces associated with this movement. Ship motions are defined in the inertial reference frame $O^0x^0y^0z^0$, while the forces are mainly defined with respect to local coordinate systems $O^ix^iy^iz^i$, which move with the ship; see Figure 5. Hereafter, the superscript characters A and B denote the striking and the struck ship, respectively. If the superscript is omitted or replaced by i, it means that the description is common to both ships.

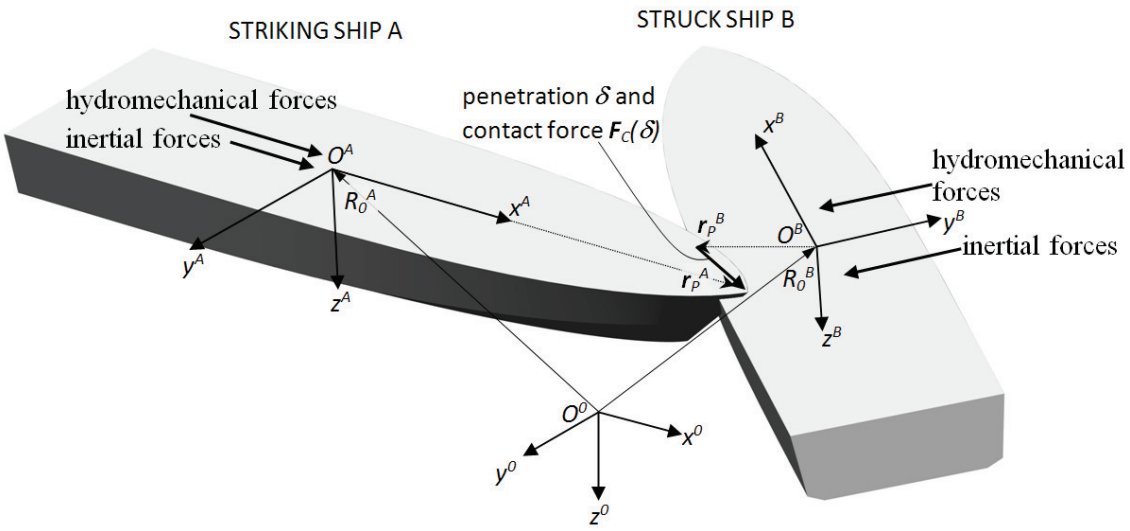

Figure 5. Definition of collision dynamics and kinematics.

During a collision, the initial kinetic energy of the ships is transferred to the work done by the ship motions and by the forces. However, to get a comprehensive overview of collision dynamics a presentation through energies is more advantageous compared to that through motions and forces. The time histories of the energy components in the symmetric large-scale collision experiments with Y-core (Wevers

and Vredeveldt, 1999) and X-core (Wolf, 2003) structures were studied in [P1]. These time histories are presented in Figure 6, including the energy E^A associated with the striking ship, E^B associated with the struck ship, and their difference, i.e. the deformation energy E_D. In these tests, the contact between the ships lasted for about 0.6 s. For the sake of comparison, the total deformation energy E_D^*, consisting of plastic and elastic components, evaluated with the decoupled approach of Minorsky (1959) is also presented in the figure. This energy is evaluated by exploiting the ships' structural and hydrodynamic added masses, as presented in Tables 1 and 2 in [P1]. With the help of this energy, a large discrepancy between the Y- and X-core tests is revealed. In the Y-core experiment, differently from the X-core one, both ships had partially filled liquid tanks on board that caused the sloshing phenomenon during the collision. This sloshing stores part of the energy and therefore there is less energy available for structural deformations. Thus, the model of Minorsky fails to predict the deformation energy in the case of the Y-core experiment, while in the case of the X-core test the prediction agrees well with the experimental value.

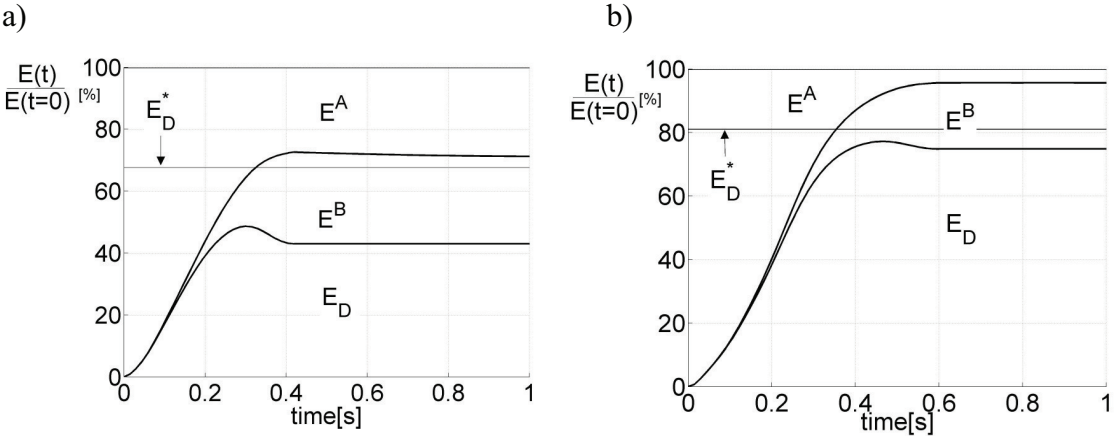

Figure 6. The time history of energy components in relative form throughout a large-scale collision with Y-core (a) and X-core (b) experiments.

To get a more detailed understanding of the physics of ship collisions, the time-histories of E^B and E^A in the Y-core collision are divided into their components in Figure 7. There, the importance of the hydrodynamic damping W_K^B and the kinetic energy E_{KIN}^B of the struck ship compared to that of the striking ship, for which W_K^A is

not even depicted, can be clearly seen. It should be noticed that the kinetic energy E_{KIN}^{B} covers both the structural mass and the hydrodynamic added mass. Furthermore, Figure 7 illustrates the transformation of the kinetic energy into sloshing energy E_{SL}^{i} during the collision. The significance of the sloshing is clearly seen in the case of the striking ship in Figure 7b, where at the time instant of the maximum contact force, around t = 0.5 s, almost all of the energy is associated with the sloshing motions of the liquid in the tanks. The energy E_{F}^{B} to overcome the hydrodynamic drag resulting from sway motion, and also the energy E_{B}^{B} caused by the dynamic bending of the hull girder, are relatively small compared to the other energy components.

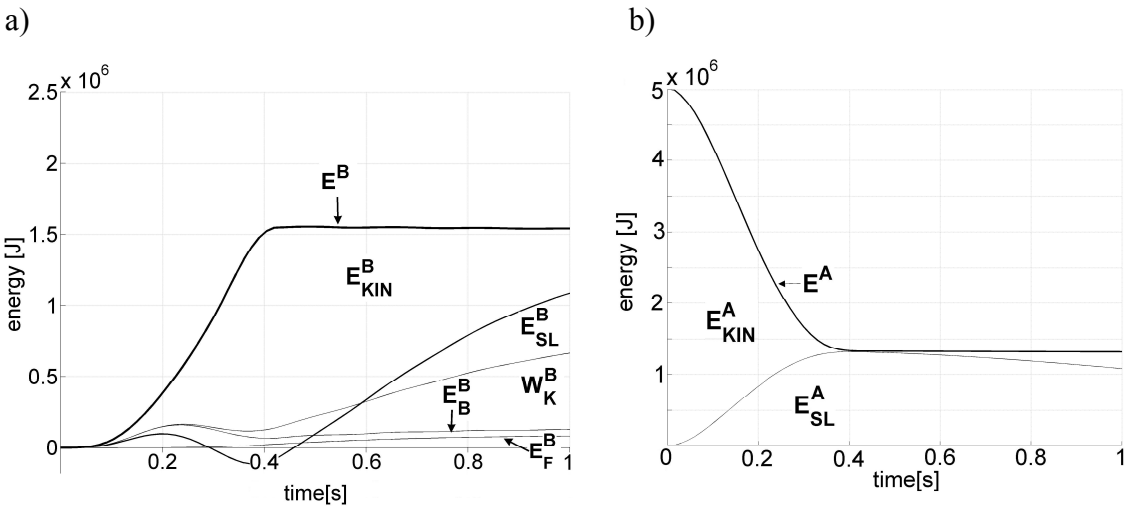

Figure 7. The variation in the motion energy components throughout the large-scale collision in the case of the struck ship (a) and the striking ship (b).

3.2. Hydromechanical forces

The hydromechanical forces, especially the radiation force, together with the ship's inertia and the contact force, are the main components in collision dynamics. An accelerating or decelerating ship encounters a hydrodynamic radiation force induced by the relative acceleration between the hull and the water. The acceleration component of this force is based on the constant added mass at an infinite frequency of motion multiplied by the ship's acceleration. In the presence of a free surface an additional force component – hydrodynamic damping – arises. This is evaluated with the help of

the convolution of the velocity and retardation function, which accounts for the memory effect of water (Cummins, 1962; Ogilvie, 1964). This approach requires the evaluation of the frequency-dependent added mass and the damping coefficients, which are calculated with the help of the strip theory (Journée, 1992).

The importance of the radiation force and the corresponding energy increases in non-symmetric collisions as a result of the longer contact duration compared to that of symmetric collisions. This is demonstrated by the time histories of the relative radiation energies in Figure 8. There, these energies are presented over the duration of the contact in model-scale tests with similar loading conditions and collision velocities. There, the kinetic energy E_μ resulting from the added mass dominates during the first half of the contact, while the work W_K^i resulting from the hydrodynamic damping becomes the most important radiation energy component by the end of the contact, where it accounts for about 17% of the total available energy in a non-symmetric collision and for about 10% in a symmetric collision.

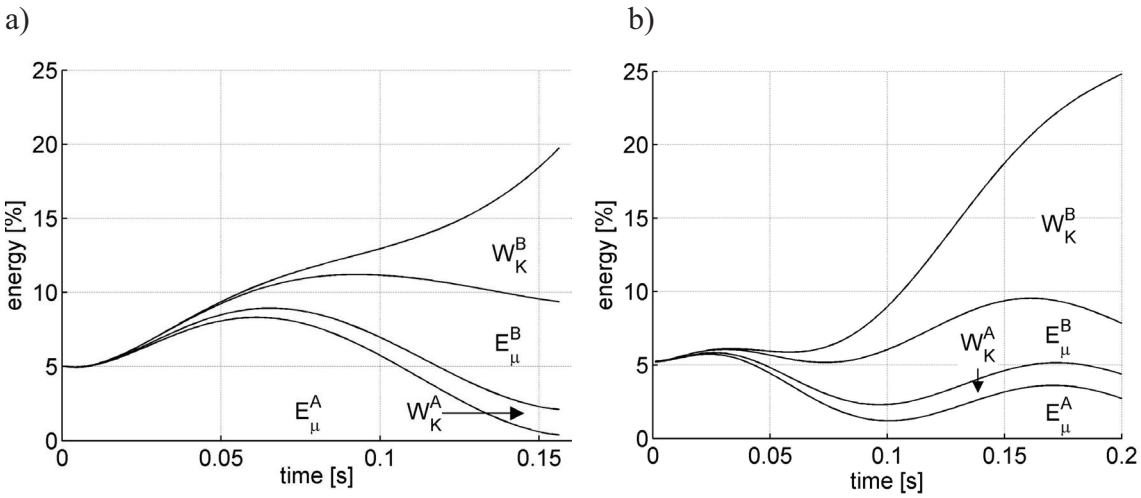

Figure 8. The proportions of the radiation energy to the total available energy in a symmetric model-scale test, No. 111 (a), and a non-symmetric model-scale test, No. 303 (b) (see Appendix B in [P3] for the test matrix).

The hydrostatic restoring force is assumed to be proportional to the angular displacement of the ship from the equilibrium position, limiting the displacement to angles of approximately 10° [P3]. The hydrodynamic drag is assumed to be proportional

to the square of the ship's velocity and is considered for surge and sway. In the surge direction only the frictional resistance is included with the ITTC-57 friction line formula, as the magnitude of the other resistance components is assumed to be negligible. The modelling of the hydrodynamic drag in the sway direction is based on the formula presented by Gale et al. (1994).

3.3. Contact between the ships

The interaction between the ships during a collision is through a contact force common to both ships. The interaction is modelled using the kinematic condition, which describes the penetration path of the contact force from the ship motions in the time domain. The penetration is solved piecewise in the time domain and then the instantaneous contact force is calculated on the basis of the geometry of the colliding bodies and using a simple model of contact mechanics relating penetration to the contact force.

As assumed in Chapter 1, all the deformations resulting from a collision are limited to the side structure of the struck ship, which deforms according to the shape of the penetrating rigid bow of the striking ship. The contact process is divided into three distinct phases [P3]. The contact starts with a loading phase, during which the penetration depth increases. This loading is followed by a short stiction phase, during which the direction of the relative velocity between the ships reverses and, thus, an unloading phase starts, during which the ships separate as a result of the elastic springback of the deformed structures.

The contact force at each time step is obtained by integrating the normal and tangential tractions over the contact surface between the colliding bodies. The shape of the contact surface is based on the geometry and the relative position of the ships. The normal traction is equal to the known maximum normal stress on the surface of the deformed side structure. The tangential traction is based on the Coulomb friction law stating the proportionality between tangential and normal traction components.

For the integration of the contact force, the contact surface is divided into integration elements. The normal traction occurs in compression and its direction is

determined by the normal of the element. However, the direction of the tangential traction depends on the relative motion between the ships. During the loading and the unloading phases this direction is determined as a projection of the relative velocity into the plane of the integration element. In the stiction phase the direction of the tangential traction is based on the relative acceleration to avoid singularity problems with the reversing velocity (Canudas et al., 1995; Dupont et al., 2000).

When the penetration starts to decrease in the unloading phase, the contact is not immediately lost because of the elastic springback of the deformed structure. This is considered throughout the unloading phase in order to define the contact surface and the direction of the relative velocity in the plane of the integration element. It was assumed in [P3] that the struck ship's structure in contact with the integration element recovers along a path defined by a normal of the initial un-deformed surface. The direction of the relative velocity on the contact surface is based on the rate of recovery along that path and this direction determines that of the tangential traction.

3.4. Dynamic hull bending

In addition to rigid body motions in sway, impact loading caused by a collision also induces the transverse dynamic bending of the hull girder of the struck ship [P1]. It is assumed that the cross-sections of the hull girder remain plane, which allows the modelling of the ship girder as an Euler-Bernoulli beam. The hull girder is modelled as a body with free end boundary conditions. There, the major physical properties are its length, flexural stiffness, mass per unit length, and internal damping.

The vibratory response of the ship hull girder is based on the superposition of its eigenmodes. These, with the corresponding eigenfrequencies, are solved according to Timoshenko et al. (1937). However, in a collision only the response resulting from the lowest eigenmode is of interest. The equation of motion of vibratory response in time domain is expressed with generalised coordinate (Clough and Penzien, 1993) exploiting the corresponding generalised loading at each time step and the generalised mass, which also includes the constant added mass in sway. The loading considers only the component of the contact force transverse to the struck ship. The value of internal

structural damping in bending is based on the measured damping values of several ships (ISSC, 1983).

3.5. Sloshing interaction

Sloshing covers a transient fluid motion inside an onboard tank caused by a rapid movement of a ship hull during a collision. The effect of the sloshing on the collision dynamics is based on time-varying loads on the tank bulkheads and, thus, causes a change in the energy distribution during a collision.

Sloshing interaction in ship collisions was studied in [P1] and [P4] on the basis of the large- and model-scale experiments, and on theoretical modelling, applying computational fluid dynamics (CFD) and the mathematical analogy model developed by Graham and Rodriguez (1952). This model is based on the linear potential flow theory, which assumes linearised free surface conditions. There, the water in a partially filled tank is divided into a rigid mass and into a finite number of oscillating masses. These oscillating masses are connected to the bulkheads by springs and viscous dampers, where the spring compression and the damper velocity give the sloshing force for the equations of motion in sway and surge. Each of these oscillating masses with damping describes one eigenmode of fluid sloshing.

To get full correspondence to the results of the potential flow theory, a mechanical model of sloshing requires an infinite number of such oscillating elements. However, it has been proven that the sloshing force induced by a spring-mass element decreases rapidly with an increasing mode number (Abramson, 1966). On the basis of the CFD calculations, it was concluded in [P1] that a sufficient number of oscillating masses is three in collision applications. The damping coefficients for the viscous damping model were evaluated by CFD calculations in [P1] and by model-scale experiments in [P4]. The damping coefficient increases as a function of the initial velocity of the striking ship and decreases with the relative filling level in the tanks.

4. Time-domain simulation model

4.1. Equations of motion and time integration

A time domain simulation of collision combines all the forces discussed in Chapter 3 in a single calculation and gives the ships' behaviour with the collision forces. The relation between the forces and the ship motions is described through a system of equations of motion for each ship. There, the contact force is derived with the help of a kinematic condition based on the relative motion between the ships. The system of six equations of rigid body motions was presented in [P3]. In [P4] this system was extended to take the sloshing into account. There, it was assumed that the effect of sloshing on the ship's mass centre is negligible and thus it remains fixed to its initial position. The transverse vibratory bending of the hull girder of the struck ship was included in [P1] as an additional equation of motion in the sway direction. All the Newtonian equations of motion are expressed in the local coordinate systems of the ships, allowing a fast evaluation of the hydromechanical and the sloshing forces.

The time integration of the equations of motion is based on an explicit 5^{th}-order Dormand-Prince integration scheme, which is a member of the Runge-Kutta family of solvers (Dormand and Prince, 1980). Inside a time integration increment, seven sub-increments are calculated. The hydrodynamic inertia force, the restoring force, the sloshing forces, and the ship motions are updated in every sub-increment. On the other hand, the contact force, velocity-dependent radiation force, and the hydrodynamic drag are kept constant during the whole integration increment for the sake of time efficiency. The results converged when the time increment was around 10 ms on a full scale.

4.2. Numerical solution procedure

The procedure of the time domain simulation is presented in Figure 9, where it is divided into three steps. First, at time t, the position, velocity, and acceleration are known for both ships. As a second step, the external forces are calculated for time t on the basis of these values. The gravity force is constant throughout the collision and acts along the global vertical axis z^0. The hydromechanical forces are calculated in a local

coordinate system from the position and motions of the ships. For the contact force the relative position and motions are presented in the local coordinate system of the striking ship, where the contact force is calculated. Given the contact force, the vibratory bending of the hull girder is evaluated. Sloshing forces ensue from the relative motion between the sloshing masses and the ship. As a final step, the values of the initial parameters are all substituted into the equations of motion, whence the values of the ship motions are solved for time instant $t+\Delta t$.

The solution of the equations of motion for both colliding ships at time instant $t+\Delta t$ provides kinematically admissible motions given in the local coordinate system $O^i x^i y^i z^i$. In addition, the vibratory response of the hull girder of the struck ship is added to the sway motion of the rigid body. The new position of the ship's centre of gravity at $t+\Delta t$ with respect to the inertial frame is evaluated by transforming the translational displacement increments to the inertial frame. After this, the orientation with respect to the inertial frame is updated by the angular increments of Euler's angles. The process is repeated until the end of the collision.

1. Known solution at time t: position, orientation, and motions
$^{t}\mathbf{x}^{i}, {}^{t}\boldsymbol{\varphi}^{i}, {}^{t}\dot{\mathbf{x}}^{i}, {}^{t}\ddot{\mathbf{x}}^{i}, {}^{t}\boldsymbol{\Omega}^{i}, {}^{t}\dot{\boldsymbol{\Omega}}^{i}$

sloshing motions $^{t}\mathbf{x}_{n}^{i}, {}^{t}\dot{\mathbf{x}}_{n}^{i}, {}^{t}\ddot{\mathbf{x}}_{n}^{i}$

hull bending response $^{t}\eta^{B}(x,t)=\phi_{i}(x)\,p(t)$

2. Calculate external forces at time t

a. *Gravity force* [P3] $\mathbf{F}_{G}$

b. *Hydrostatic buoyancy force* [P3] $\mathbf{F}_{B}$

c. *Hydrodynamic forces*

(i) frictional resistance and hydrodynamic drag [P3] $\mathbf{F}_{F}$

(ii) hydrodynamic radiation force [P3] $\mathbf{F}_{\mu}(t)+\mathbf{F}_{K}(t)$

d. *Contact force* $\mathbf{F}_{C}^{A}=-\mathbf{F}_{C}^{B}=\mathbf{F}_{p}^{A}+\mathbf{F}_{q}^{A}$

(i) compressive force [P3] $\mathbf{F}_{p}^{A}$

(ii) friction force [P3] $\mathbf{F}_{q}^{A}$

e. *Dynamic hull bending: generalised force* [P1] q_{i}^{*}

f. *Sloshing interaction* [P4]

$$\left[\mathbf{C}_{n}\right]\left({}^{t}\{\dot{\mathbf{x}}\}^{T}\quad {}^{t}[\Omega]^{T}\quad {}^{t}\{\dot{\mathbf{x}}\}_{n}^{T}\right)+\left[\mathbf{K}_{n}\right]\left({}^{t}\{\mathbf{x}\}^{T}\quad [\boldsymbol{\varphi}]^{T}\quad \{\mathbf{x}_{n}\}^{T}\right)$$

3. Solve the equations of motion for t+Δt

a. *Equation of motions (EOM)* (**F**- force, **G**- moment of forces) [P3]

$$\left[\mathbf{M}_{\mu}\right]\begin{Bmatrix}\dot{\mathbf{u}}\\ \dot{\boldsymbol{\Omega}}\end{Bmatrix}+\left[\mathbf{M}_{\mu}^{\Omega}\right]\begin{Bmatrix}\mathbf{u}\\ \boldsymbol{\Omega}\end{Bmatrix}-\mathbf{F}_{R}=\begin{Bmatrix}\mathbf{F}\\ \mathbf{G}\end{Bmatrix}-\mathbf{F}_{\mu}-\mathbf{F}_{R}$$

b. *EOM in the case of complementary effects* [P1] & [P4]

$$\begin{cases}\left(\begin{bmatrix}\left[\mathbf{M}_{\mu}\right] & [0]\\ [0] & [0]\end{bmatrix}+\left[\mathbf{M}_{n}\right]\right)\begin{Bmatrix}\dot{\mathbf{u}}\\ \dot{\boldsymbol{\Omega}}\\ \dot{\mathbf{u}}_{n}\end{Bmatrix}+\left(\begin{bmatrix}\left[\mathbf{M}_{\mu}^{\Omega}\right] & [0]\\ [0] & [0]\end{bmatrix}+\left[\mathbf{C}_{n}\right]\right)\begin{Bmatrix}\mathbf{u}\\ \boldsymbol{\Omega}\\ \mathbf{u}_{n}\end{Bmatrix}+\left[\mathbf{K}_{n}\right]\begin{matrix}\{\mathbf{x}\}\\ [\boldsymbol{\varphi}]\\ \{\mathbf{x}_{n}\}\end{matrix}=\begin{Bmatrix}\mathbf{F}\\ \mathbf{G}\end{Bmatrix}-\mathbf{F}_{\mu}, \\ m_{1}^{*B}\ddot{p}_{1}(t)+2\xi\omega_{1}^{B}m_{1}^{*B}\dot{p}_{1}(t)+\left(\omega_{1}^{B}\right)^{2}m_{1}^{*B}p_{1}(t)=q_{1}^{*B}(t)\end{cases}$$

Solution of equations of motions of ships' response at time t+Δt

$$^{t+\Delta t}\mathbf{x}^{i}, {}^{t+\Delta t}\boldsymbol{\varphi}^{i}, {}^{t+\Delta t}\dot{\mathbf{x}}^{i}, {}^{t+\Delta t}\ddot{\mathbf{x}}^{i}, {}^{t+\Delta t}\boldsymbol{\Omega}^{i}, {}^{t+\Delta t}\dot{\boldsymbol{\Omega}}^{i}, {}^{t+\Delta t}\mathbf{x}^{i}, {}^{t+\Delta t}\dot{\mathbf{x}}^{i}, {}^{t+\Delta t}\ddot{\mathbf{x}}^{i}, {}^{t+\Delta t}\eta^{B}(x)$$

Notations: $[\mathbf{M}_{\mu}]$ mass and inertia matrix, also including added masses; $\left[\mathbf{M}_{\mu}^{\Omega}\right]$ matrix of non-linear acceleration and mass and inertia terms, also including added masses; $\left[\mathbf{M}_{n}\right]$ matrix of sloshing masses; $\left[\mathbf{C}_{n}\right]$ matrix of damping coefficients for sloshing; $\left[\mathbf{K}_{n}\right]$ matrix of stiffness coefficients for sloshing; m_{1}^{*B} generalised mass; ω_{1}^{B} lowest eigenfrequency of the hull girder; ξ internal damping of the hull girder; { } vector; [ ] matrix

Figure 9. Solution process of time-domain simulations.

4.3. Comparison to a momentum conservation model

The deformation energies and penetration paths of the contact force are calculated for four non-symmetric model-scale collision tests using both the developed time-domain simulation model and a decoupled approach based on the momentum conservation law. A calculation model based on the momentum conservation gives as an output only the energy absorbed by structural deformations. Here, the decoupled model of Zhang (1999) is exploited to evaluate this energy, and in Table 1 it is compared to the energies obtained from the model-scale experiments and by the present coupled approach. For the decoupled model only the total deformation energy is presented, while for the other two methods the pure plastic deformation energy is also presented. In the decoupled model the decomposition of the total energy into its plastic and elastic components requires a knowledge of the ships' velocities immediately after the contact, which cannot be precisely defined on the basis of the decoupled approach alone.

Table 1. Deformation energy obtained by different methods (total deformation energy/plastic deformation energy)

Test	Experimental (total/plastic) [J]	Decoupled model (Zhang, 1999) [J]	Coupled model (total/plastic) [J]
202	2.36/2.28	2.48/-	2.51/2.14
301	4.20/4.14	4.30/-	4.62/4.21
309	3.19/3.19	4.4(2.9*)/-	3.60/3.60
313	3.14/3.09	3.7/-	3.45/3.14

*- deformation energy assuming sliding contact in Zhang's model

Computational models tend to overestimate the total deformation energy by approximately 10% and both methods give a similar outcome, except in Test No. 309, where there is significant sliding between the ships. The plastic deformation energy evaluated with the coupled approach agrees well with the experimental measurements.

In the decoupled model the total deformation energy is the only outcome and the penetration is assumed to follow the direction of the initial velocity of the striking ship

(Zhang, 1999). To solve the final value of the penetration corresponding to the deformation energy obtained, the contact force model from [P3] is exploited.

a) 202 (β=90 deg, L_C=0.83 m)

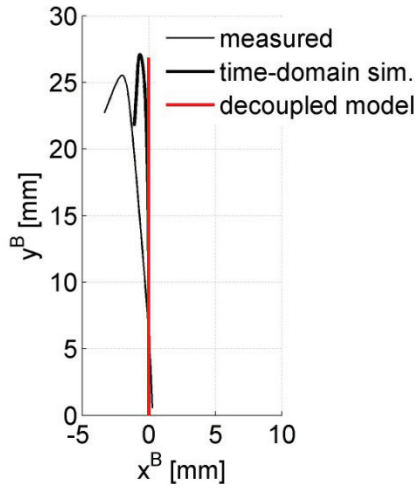

b) 301 (β=120 deg, L_C=0.37 m)

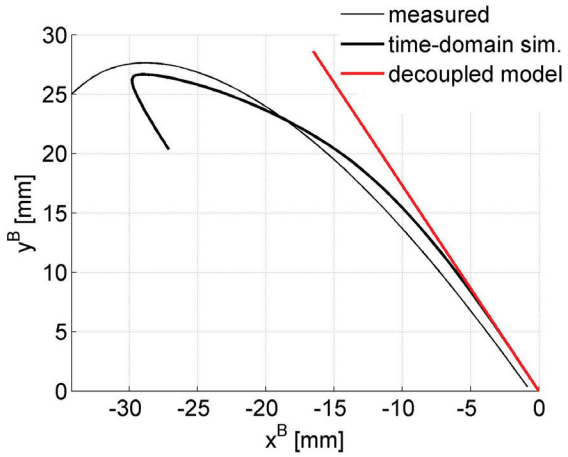

c) 309 (β=145 deg, L_C=0.46 m)

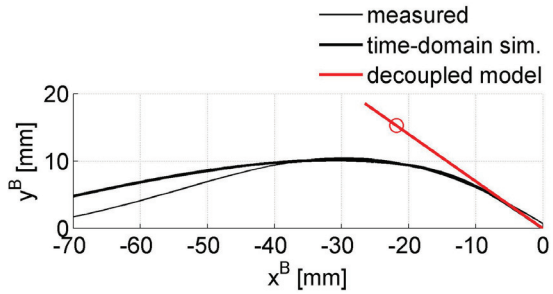

d) 313 (β=60 deg, L_C=0.29 m)

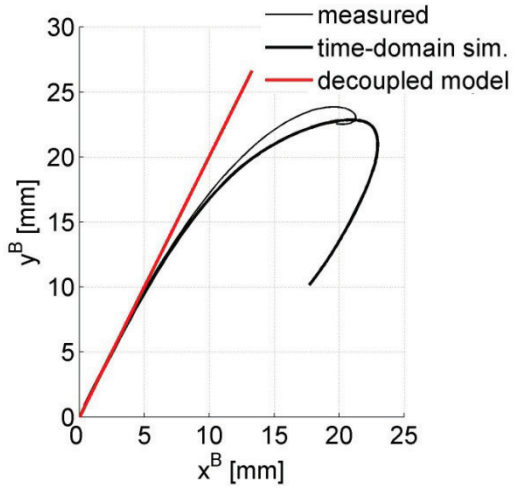

Figure 10. Penetration paths of the bulb in the struck ship (see Appendix B in [P3] for test matrix).

The penetration paths evaluated by two computational models are presented in Figure 10. There, the penetration paths of the bulb into the side of the struck ship are presented. The longitudinal extent of the damage is denoted by x^B and, correspondingly, the transverse extent by y^B. For Test No. 202, presented in Figure 10a, the results of

both methods agree well with the measured one, even though the longitudinal penetration is slightly underestimated. In other tests with an oblique angle the differences between the results obtained with the different methods are larger. The developed method estimates the penetration paths with good accuracy, but the decoupled approach yields a deeper penetration, while the longitudinal extent of the damage is smaller. This becomes especially clear from the results of Test No. 309 in Figure 10c, where the striking ship slides along the side of the struck ship and thus the penetration path deviates significantly from the direction of the initial velocity. A circular marker in Figure 10c denotes the deformation energy when the sliding contact is assumed to occur in the model of Zhang (1999).

5. Conclusions

The dynamics of ship collisions have been studied experimentally on a large and on a model scale. The experimental observation gave valuable information for the basic assumptions in the 3D time-domain simulation model for collisions that was developed. There, the ship motions and the contact force are treated simultaneously and all the major external forces acting on the ships during a collision are considered at a reasonable level of accuracy. The analyses of the large-scale collision experiments revealed that the existing simulation tools did not include all the relevant effects. Therefore, the simulation model that was developed also considers some complementary effects, such as sloshing and the vibratory bending of the hull girder in the transverse direction.

Both the experiments and the simulations emphasised the importance of the coupling between the motions and the contact force, which resulted in a complex motion kinematics that could not be handled on the basis of the initial input parameters of the collision alone. It became especially obvious in the case of non-symmetric collisions, where the penetration paths were heavily dependent on the actual ship motions during the collision and on the structural properties of the ships. The penetration paths calculated with the time-domain simulation model agreed well with those from the large- and model-scale experiments, while the decoupled approach predicted, as expected, penetration that was too deep and short. However, both the coupled and decoupled approaches were able to predict the total deformation energy with a deviation of about 10%. On the basis of the model tests it can also be concluded that the hydrodynamic coupling between the colliding ships caused slightly higher penetration in the vertical direction, compared to that predicted with the time-domain simulations. The elastic springback of the deformed structures of the struck ship became important when the unloading phase was modelled. While in symmetric collisions there is a clear shift from the loading to the unloading at the time instant of the maximum contact force and penetration, in non-symmetric collisions the unloading starts in some regions of the contact surface before the maximum penetration occurs. Thus, in these scenarios the elasticity also plays an important role in predicting the maximum

penetration. Furthermore, the hydrodynamic radiation forces acting on the colliding ships proved to have a strong influence on the energy distribution as at the end of the contact they accounted for up to 25% of the total available energy. However, if the interest is in the maximum collision force and penetration depth, then the approach based on the constant added mass and ignored hydrodynamic damping is still reasonable, as the error in the deformation energy is about 5%. The energy absorbed to overcome the hydrodynamic drag accounts for about 1%-2% of the total energy.

The results of the large- and model-scale experiments with partially filled liquid tanks emphasised the importance of sloshing for collision dynamics. The structural deformation energy in the wet tests was only about 70%-80% of that in similar dry collision tests. This energy reduction is strongly affected by the amount of sloshing water, while the effect of the collision speed is of secondary importance. The simulation method that was developed with the Graham and Rodriguez linear sloshing model overestimated the deformation energy by up to 10% in the case of the wet model-scale tests, but in the case of the large-scale wet test the predictions agreed amazingly well. The overestimation in the model-scale tests was due to the low relative filling levels of water and thus, the linear sloshing model is close to the boundary of its validity. Therefore, it can be concluded that this linear sloshing model gives results which are completely satisfactory within a certain range of water depths. The vibratory bending of the hull girder contributed to the sway velocity and acceleration at the amidships of the struck ship; however, its contribution to the energy balance is small, around 1%-2% of the total energy.

The model developed here can be used to estimate the deformations in non-symmetric collisions or when the ships are prone to sloshing in collision. However, the contact model should be extended to consider ship-like side structures, which have more complex deformation mechanisms in comparison to the one used in the simulations of the model-scale experiments. This, together with motion simulations, would improve the accuracy of collision analyses and, thus, allow the crashworthiness of different structural arrangements to be increased. More advanced sloshing models could enlarge the validity range of the sloshing and even include the different geometries and structural arrangements inside the tanks.

6. References

Abramson, H.N. Analytical representation of lateral sloshing by equivalent mechanical models, the dynamic behaviour of liquids in moving containers. NASA SP-106. Washington, USA, 1966, pp. 199-223.

Amdahl, J., Kavlie, D. Experimental and Numerical Simulations of Double Hull Stranding. DNV-MIT Workshop on Mechanics of Ship Collision and Grounding. Norway, 1992.

Broekhuijsen, J. Ductile failure and energy absorption of Y-shape test section. Master's Thesis, Delft University of Technology, Netherlands, 2003, p. 90.

Brown, A. Collision scenarios and probabilistic collision damage. Journal of Marine Structures, 2002, Vol. 15, pp. 335-364.

Canudas de Wit, C., Olsson, H., Åström, J., Lischinsky, P. A new model for control of systems with friction. IEEE Transactions Automatic Control, 1995, Vol. 40, pp. 419-425.

Carlebur, A.F.C. Full-scale collision tests. Safety Science, 1995, Vol. 19, pp. 171-178.

Clayton, B.R., Bishop, R.E.D. Mechanics of Marine Vehicles, E. F. N. Spon Ltd, London, 1982, p. 597.

Clough, R.W., Penzien, J. Dynamics of Structures. McGraw-Hill Book Company, 2nd edition, New York, 1993, p. 740.

Cummins, W.E. The Impulse Response Function and Ship Motions. Schifftechnik, 1962, Vol. 9, pp. 101-109.

Dormand, J.R., Prince, P.J. A family of embedded Runge-Kutta formulae. Journal of Computational and Applied Mathematics, 1980, Vol. 6, pp. 19-26.

Drittler, K. Die Bestimmung von hydrodynamischen Kenngrösen bei Schiffbewungen parallel zur Wasseroberfläche und bei Kollisionen. Schifftechnik, 1966, Vol. 13, pp. 63-69.

Dupont, P., Amstrong, B., Hayward, V. Elasto-Plastic Friction Model: Contact Compliance and Stiction. In: Proceedings of the American Control Conference, Chicago: AACC, 2000, pp. 1072-1077.

Eliopoulou, E., Papanikolaou, A. Casualty analysis of large tankers. Journal of Marine Science and Technology, 2007, Vol. 12, pp. 240-250.

Gale, C., Eronen, H., Hellevaara, M., Skogman, A. Perceived Advantages of Z-Drive Escort Tugs. In: Proceedings of the International Towage and Salvage Convention, Southampton, 1994, pp. 163-176.

Graham, E.W., Rodriguez, A.M. The Characteristics of Fuel Motion Which Affect Airplane Dynamics. Journal of Applied Mechanics, 1952, Vol. 19, pp. 381-388.

ISSC. Steady state loading and response. Report of Committee II.4. Proceedings of the 8th International Ship Structures Congress, 1983, p. 64.

Journée, J.M.J. Strip theory algorithms. Delft University of Technology; Report MEMT 24, 1992.

Kitamura, O. Buffer Bow Design for the Improved Safety of Ships. In: Proceedings of the Ship Structure Symposium, 2000.

Konter, A., Broekhuijsen, J., Vredeveldt, A. A quantitative assessment of the factors contributing to the accuracy of ship collision predictions with the finite element method. In: Proceedings of 3rd International Conference on Collision and Grounding of Ships, Japan, 2004, pp. 17-26.

Lax, R. Simulation of Ship Motions in Grounding (in Finnish). Helsinki University of Technology, Report M-260, 2001, p. 129 +app.

Le Sourne, H., Donner, R., Besnier, F., Ferry, M. External Dynamics of Ship-Submarine Collision. In: Proceedings of 2nd International Conference on Collision and Grounding of Ships, Denmark, 2001, pp. 137-144.

Ludolphy, J.W.L., Boon, B. Collision resistant side shell structures for ships. In: Proceedings of IMDC-2000, Korea. 2000.

Lützen, M. Ship Collision Damage. Ph.D. Thesis, Technical University of Denmark, 2001.

Minorsky, V.U. An analysis of ship collision with reference to protection of nuclear power plants. Journal of Ship Research, 1959, Vol. 3, pp. 1-4.

Motora, S., Fujino, M., Suguira, M., Sugita, M. Equivalent added mass of ships in collision. Selected papers from J Soc. Nav. Archit., Japan, 1971, Vol. 7, pp. 138-148.

Määttänen, J. Experiments on Ship Collisions in Model Scale. Master's Thesis, Helsinki University of Technology, 2005. p 145.

Ogilvie, T.F. Recent Program Towards the Understanding and Prediction of Ship Motions. In: Proceedings of 5th Symposium on Naval Hydrodynamics, Norway, 1964, pp. 3-128.

Pedersen, P.T., Zhang, S. On Impact Mechanics in Ship Collisions. Journal of Marine Structures, 1998, Vol. 11, pp. 429-449.

Pedersen, P.T., Li, Y. On the global ship hull bending energy in ship collisions. In: Proceedings of 3rd International Conference on Collision and Grounding of Ships, Japan, 2004, pp. 1-6.

Petersen, M.J. Dynamics of Ship Collisions. Journal of Ocean Engineering, 1982, Vol. 9, pp. 295-329.

Ranta, J., Tabri, K. Study on the Properties of Polyurethane Foam for Model-Scale Ship Collision Experiments. Helsinki University of Technology, Report M-297, 2007, p. 44.

Smiechen, M. Zur Kollisiondynamic von Schiffen. Jb. Schiffbautech. Ges, 1974, Vol. 68, pp. 357-372.

Soininen, H. Study on a collision barrier of a nuclear icebreaker, in Finnish. Helsinki University of Technology, Licentiate Thesis, 1983. p. 114.

Tabri, K., Broekhuijsen, J., Matusiak, J., Varsta, P. Analytical Modelling of Ship Collision Based on Full Scale Experiments. In: Proceedings of 3rd International Conference on Collision and Grounding of Ships, Japan, 2004, pp. 302-311.

Tasai, F. Hydrodynamic force and moment produced by swaying and rolling oscillation of cylinders on the free surface. Rep. on Research Inst. for Applied Mech., Kyushu University, 1961, Vol. 9, No. 35.

Timoshenko, S.P., Young, D.H, Weaver, W. Vibrations Problems in Engineering, 2nd edition. D. Van Nostrand Company Inc, New York, 1937.

Tuovinen, J. Statistical Analysis of Ship Collisions. Master's Thesis, Helsinki University of Technology, 2005, p. 93.

Vugts, J.H. The hydrodynamical coefficients for swaying, heaving and rolling cylinders in a free surface. Netherlands Ship Research Centre TNO, Report No.112 S, 1968, p. 31.

Wevers, L.J., Vredeveldt, A.W. Full Scale Ship Collision Experiments 1998. TNO-report 98-CMC-R1725, Netherlands, 1999, p. 260.

Woisin, G. Design against collisions. Schiff & Hafen, 1979, Vol. 12, pp. 1059-1069.

Woisin, G. Instantaneous Loss of Energy with Unsymmetrical Ship Collisions. Schiff & Hafen, 1988, Vol. 40, pp. 50-55.

Wolf, M. Full scale collision experiment, X-type Sandwich side hull. EU Sandwich project report Deliverable TRD448, 2003, p. 21.

Zhang, S. The mechanics of ship collisions. Ph.D. thesis, Technical University of Denmark, 1999, p. 262.

Zhang, A., Suzuki, K. A comparative study of numerical simulations for fluid structure interaction of liquid-filled tank during ship collision. Journal of Ocean Engineering, 2007, Vol. 34, pp. 645-652.

ISBN 978-952-248-272-3
ISBN 978-952-248-273-0 (PDF)
ISSN 1795-2239
ISSN 1795-4584 (PDF)